CISTER
Research Centre in
Real-Time & Embedded
Computing Systems

Conference Paper

In-Tunnel Multi-Ray Analysis for Los V2V Links with Multiple Antennas

Miguel Gutiérrez Gaitán
Ramiro Robles

CISTER-TR-210404

2021/06/14

In-Tunnel Multi-Ray Analysis for Los V2V Links with Multiple Antennas

Miguel Gutiérrez Gaitán, Ramiro Robles

CISTER Research Centre

Polytechnic Institute of Porto (ISEP P.Porto)

Rua Dr. António Bernardino de Almeida, 431

4200-072 Porto

Portugal

Tel.: +351.22.8340509, Fax: +351.22.8321159

E-mail: mjggt@isep.ipp.pt, rsr@isep.ipp.pt

https://www.cister-labs.pt

Abstract

This paper presents a geometric multi-ray tracing analysis for vehicle-to-vehicle (V2V) communication in tunnel environments. The objective is to investigate the performance of V2V MIMO (multiple input multiple-output) antenna systems in the presence of multiple (specular) reflections inside a tunnel, e.g. from ground, walls and ceiling. To this purpose, we built upon our prior work where we established the V2V MIMO channel with ground reflections as an extension of the classical two-ray model. Then, in line with this vision, we increased the number of potential reflected rays to those dominating the particular tunnel's geometry. We assessed the performance of the in-tunnel V2V MIMO link assuming transmit symbols repetition and different receiver combining schemes. Analytical results for a semicircular tunnel reveals that multiple antenna systems can be useful to exploit/counteract the constructive/destructive interference patterns typically observed in tunnel-like surroundings.

In-Tunnel Multi-Ray Analysis for LOS V2V Links with Multiple Antennas

Miguel Gutiérrez Gaitán[‡†*] and Ramiro Sámano-Robles[*]
[*]CISTER Research Centre, ISEP, Politécnico do Porto, Portugal – {mjggt,rasro}@isep.ipp.pt
[†]CISTER Research Centre, FEUP, Universidade do Porto, Portugal
[‡]Facultad de Ingeniería, Universidad Andres Bello, Santiago, Chile

***Abstract*—This paper presents a geometric multi-ray tracing analysis for vehicle-to-vehicle (V2V) communication in tunnel environments. The objective is to investigate the performance of V2V MIMO (multiple-input multiple-output) antenna systems in the presence of multiple (specular) reflections inside a tunnel, e.g. from ground, walls and ceiling. To this purpose, we built upon our prior work where we established the V2V MIMO channel with ground reflections as an extension of the classical two-ray model. Then, in line with this vision, we increased the number of potential reflected rays to those dominating the particular tunnel's geometry. We assessed the performance of the in-tunnel V2V MIMO link assuming transmit symbols repetition and different receiver combining schemes. Analytical results for a semicircular tunnel reveals that multiple antenna systems can be useful to exploit/counteract the constructive/destructive interference patterns typically observed in tunnel-like surroundings.**

***Index Terms*—LOS, MIMO, Tunnel, Two-ray model, V2V**

I. Introduction

Tunnels constitute a present-day goal for vehicle-to-vehicle (V2V) channel modelling [1]. Initial work on V2V channels mostly focused on conventional propagation surroundings, often derived from typical cellular classification, e.g. urban, suburban, rural. More specific settings such as overpasses [2], parking garages [3] and in particular, tunnels [4], were added only recently. The distinctive characteristics of the tunnel infrastructure, e.g., ceiling, walls, etc., can notably influence propagation. This has attracted recent attention, particularly in the context of autonomous vehicles [5], [6].

Multipath propagation is one of the most detrimental issues of reliability of V2V links in tunnel environments [7], [8]. The operational frequency, antenna polarization, and the size and shape of the tunnel, are some of the elements to take into account when aiming at mitigating multipath. V2V channel models that examine scattering [8], reflections on the ground [9], reflections on the vehicles and/or traffic signs, etc., can complement the understanding of the in-tunnel propagation scenario. Theoretical approaches which consider many (or all) of those details are yet scarce, especially when the analysis is extended to multiple-input multiple-output (MIMO) systems. MIMO theory has been studied in depth over the last decades [10], largely focusing on the ability of the system of counteracting stochastic fading. Yet, aspects such the presence of strong (specular[1]) reflections in the line-of-sight (LOS) MIMO channel are often left aside.

In this paper, we present a geometric multi-ray analysis for LOS V2V MIMO links in tunnel environments. The analysis is useful as a tool to evaluate the performance of the links in the presence of multiple (specular) reflections inside a tunnel, e.g., from ground, walls and ceiling. The system considers multiple transceiver antennas distributed across the surface of two vehicle ends. The vehicles are assumed to communicate in LOS within the boundaries of a tunnel of an arbitrary shape. The analysis is built upon our prior work in [9] where we established V2V MIMO model as an extension of the classical two-ray propagation model. This prior work is here extended to consider an increased number of potential signal reflections, e.g., from ground, walls and ceiling. The analysis is then reduced to those reflected rays manifesting specular behavior. The systems is evaluated assuming transmit symbol repetition and different receiver combining schemes, namely equal-gain combining and maximum-ratio combining (EGC and MRC, respectively). Analytical results for a semicircular tunnel geometry reveals that ECG and MRC are both effective in mitigating the destructive self-interference patterns derived from the multiple specular reflection conditions. Additional simulation results suggest that an antenna selection approach can be used as a dominant solution to mitigate (deep) fades, and thus to further improve the reliability of the channel.

The rest of the paper is organized as follows. Section II presents an overview related works. Section III describes the scenario and the signal reception model for V2V links with multiple antennas inside a tunnel. Section IV provides the general MIMO model. Section V introduces specific antenna processing algorithms. Section VI presents the numerical results for the simulations. Section VII draws the conclusions.

II. Related work & Motivation

In recent years, many channel models have been proposed for V2V communication considering different propagation surroundings [1], [11]. The span of works is broad, including theoretical and empirical studies which consider either stochastic and/or deterministic channel conditions. The amount and variety of research work is well justified since using a

[1]i.e., when the angles of the incident ray and the reflected ray are equal.

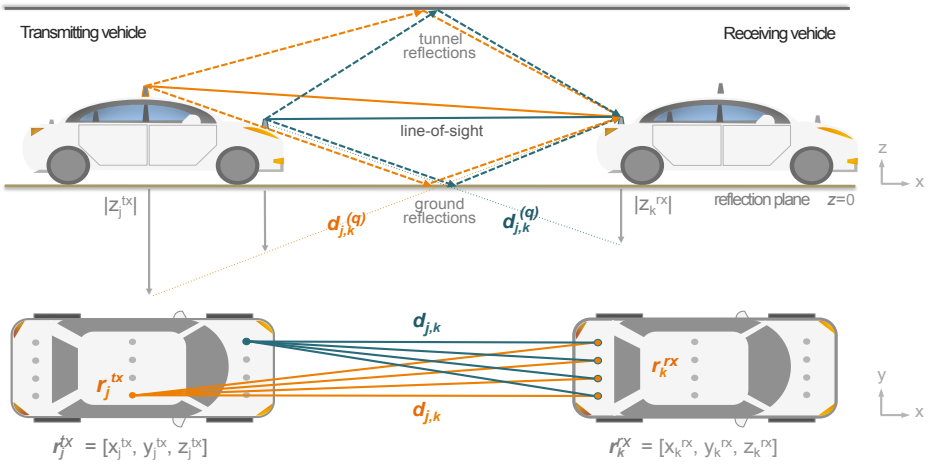

Fig. 1: V2V MIMO link inside a tunnel showing: (top) both the LOS and reflection components that the signals from two transceivers mounted on the transmitting vehicle (left) follow when sent to another transceiver on the receiving vehicle (right); and (bottom) an aerial view of the V2V LOS components.

single channel model to describe all the different V2V environments and circumstances is neither feasible nor realistic.

The more specific road settings such as overpasses, parking garage, tunnels, etc., need for apposite (often ad-hoc) studies to determine the predominant channel characteristics. Identifying those key features is crucial to improve the accuracy and simplicity of the models, especially when looking to complement the more general ones. Particularly, in tunnels, the presence of multiple reflections is a dominant propagation condition. The authors in [4] show empirical evidence of this, by reporting reflections on the walls, ceiling and ventilation systems as the most relevant. Measurements in [12] shows agreement on those reflection components, while also noting the influence of the ground plane. The research done in [13] discuss how the width and height of the tunnel have impact on the magnitude of the reflected rays, thus suggesting the existence of a close relationship between reflections dominance and tunnel shape. Theoretical details from the perspective of specular components are less explored but can be found, e.g., in [14], [12].

In this work, we assess the impact of the multiple (specular) reflections on the LOS V2V MIMO channel inside a tunnel of arbitrary shape. To the best of our knowledge, this analysis has not been carried out from a deterministic viewpoint, especially when considering multiple antennas distributed across the surface of the two vehicles. The analysis is built upon our prior work in [9], yet considering higher-order reflections due to the tunnel infrastructure. Analytical results for a semicircular tunnel geometry reveals that the conventional ECG and MRC are effective in counteracting deep fades, thus mitigating the strong specular reflection conditions inside a tunnel.

III. System Model

A. Scenario

Consider the V2V distributed antenna model depicted in Fig. 1 inside a tunnel with an arbitrary horizontal section. Each vehicle can host multiple antennas in different positions, usually on the rooftop or on the sides of the chassis. The objective of placing multiple antenna transceivers over different locations of a vehicle is to achieve diversity and thus help in reducing the effect of destructive interference that is commonly seen in links with multiple reflected components. In all cases, we consider both vertically, horizontal and cross-polarization performance. The number of Tx antennas is denoted by N_{Tx}, while the number of receive antennas is denoted by N_{Rx}. The position of the j^{th} transmit antenna is denoted by the vector $\mathbf{r}_j^{tx} = [x_j^{tx}, y_j^{tx}, z_j^{tx}]$ while the position of the k^{th} receive antenna is denoted by $\mathbf{r}_k^{rx} = [x_k^{rx}, y_k^{rx}, z_k^{rx}]$. The direct distance between antenna j in the transmitter and antenna k in the receiver is denoted by $d_{j,k}$ and is given by:

$$d_{j,k} = |\mathbf{r}_j^{tx} - \mathbf{r}_k^{rx,}|, \tag{1}$$

which, in Cartesian coordinate system, boils down to $d_{j,k} = \sqrt{(x_j^{tx} - x_k^{rx})^2 + (y_j^{tx} - y_k^{rx})^2 + (z_j^{tx} - z_k^{rx})^2}$. The distance for the q^{th} reflection is given by:

$$d_{j,k}^{(q)} = |\mathbf{r}_j^{tx} - \tilde{\mathbf{r}}_{k,q}^{rx}| = |\tilde{\mathbf{r}}_{j,q}^{tx} - \mathbf{r}_k^{rx}|, \tag{2}$$

where the notation $\tilde{\mathbf{a}}$ indicates the mirror image of vector $\mathbf{a}$ over the plane of reflection. This means that: $\tilde{\mathbf{r}}_{j,q}^{tx} = \mathbf{r}_{j,q||}^{tx} - \mathbf{r}_{j,q-}^{tx}$, where $\mathbf{r}_{j,q||}^{tx}$ and $\mathbf{r}_{j,q-}^{tx}$, denote, respectively, the parallel and perpendicular component of vector $\mathbf{r}_j^{tx}$ with respect to the reflection plane of the q^{th} reflected ray. The ground reflected component has the index $q = 0$. Since we define the ground reflection plane as $z = 0$ (see Fig.1), then $\mathbf{r}_{j,0||}^{tx} = [x_j^{rx}, y_j^{rx}, 0]^T$ and $\mathbf{r}_{j,0-}^{tx} = [0, 0, z_j^{tx}]^T$. Therefore, the expression in (2) becomes $d_{j,k}^{(0)} = \sqrt{(x_j^{tx} - x_k^{rx})^2 + (y_j^{tx} - y_k^{rx})^2 + (z_j^{tx} + z_k^{rx})^2}$. For simplicity, we do not consider additional reflections due to the body of the vehicles.

B. Channel model

The channel between the j^{th} Tx antenna and the k^{th} Rx antenna is denoted by $h_{j,k}$ and will be defined as the contribution of the line-of-sight (LOS) component and the non-line-of sight (NLOS) component, $h_{j,k} = h_{j,k}^{LOS} + h_{j,k}^{NLOS}$. Then, for convenience, we focus our analysis on the LOS component in order to evaluate the performance of distributed MIMO solutions to counteract the destructive (self-) interference of the multiple ray components.

All channels will be described by a multi-ray model. We consider the exact formulation of different plane waves travelling different distances and concurring in the same destination point. Each ray experiences an attenuation proportional to the inverse of the squared distance (path loss exponent equal to two) and a phase-shift proportional to the distance of each trajectory. This model assumes the multiple rays arrive within the boundaries of a symbol duration and we also include the values of Tx power and antenna gain for convenience in future calculations. This can be expressed mathematically as follows [15]:

$$h_{j,k}^{LOS} = \frac{\sqrt{P_T G_T G_R}}{4\pi}\left(\frac{e^{2\pi i \tilde{d}_{j,k}}}{\tilde{d}_{j,k}} + \sum_q \Gamma_q \frac{e^{2\pi i \tilde{d}_{j,k}^{(gr)}}}{\tilde{d}_{j,k}^{(gr)}}\right) \quad (3)$$

where $\tilde{d}_{j,k} = d_{j,k}/\lambda$ and $\tilde{d}_{j,k}^{(q)} = d_{j,k}^{(q)}/\lambda$, are respectively, the direct and the reflected electric distances, Γ_q is the reflection coefficient, G_T and G_R are the gains of the Tx and Rx antennas, respectively, λ is the operational wavelength and $i = \sqrt{-1}$. The reflection coefficient can be written as follows (modification of [16]):

$$\Gamma_q = \frac{A_q \sin\beta_q + B(\sqrt{n_{r,q}^2 - \cos\beta_q{}^2} + i n_{i,q})}{n_{r,q}^2 \sin\beta_q + (\sqrt{n_{r,q}^2 - \cos\beta_q{}^2} + i n_{i,q})}, \quad (4)$$

where $A_q = n_{r,q}^2$ and $B = 1$ for vertical polarization and $A_q = 1$ and $B = -1$ for horizontal polarization. β_q is the angle of reflection of the q^{th} ray, $n_{r,q}$ is the real part of the complex refractive index n_q and $n_{i,q}$ is the imaginary part of n_q, so $n_q = n_{q,r} + i n_{i,q} = \sqrt{\epsilon_{r,q} - i\frac{\sigma_q \lambda}{\epsilon_0 2\pi c}}$. c is speed light, while $\epsilon_{r,q}$ and σ_q denote, respectively, the relative permittivity and conductivity of the q^{th} reflection plane. We consider dielectric properties of asphalt [17] for the floor and of concrete blocks for the tunnel walls (as in [12]).

C. Tunnel model

In this paper we consider the reflection on the inner walls of a tunnel as rays of a V2V model based on MIMO. The tunnel is assumed to be cylindrical in the x-axis direction with a profile that can have an arbitrary boundary described by the function $f_z(y)$ which is assumed to be continuous in the range $(-R, R)$ (see Fig. 2). The normalized vector normal to the surface of the inner wall of the tunnel is thus given by:

$$\hat{\mathbf{n}} = \frac{[0 \quad 1 \quad df_z(y)/dy]}{\sqrt{1 + (df_z(y)/dy)^2}},$$

where $df_z(y)/dy$ is the first order derivative of the tunnel profile function. The condition for reflection between two antennas of contiguous vehicles is given as en extension of Snell's law as follows:

$$\mathbf{r}_j^{tx} \cdot \hat{\mathbf{n}} = \mathbf{r}_k^{rx} \cdot \hat{\mathbf{n}}, \quad (5)$$

where $\mathbf{a} \cdot \mathbf{b}$ denotes the inner product vector operation for any $\mathbf{a}$ and $\mathbf{b}$ vectors. Since the normal vector to the tunnel surface has only y and z components, the reflection condition applies

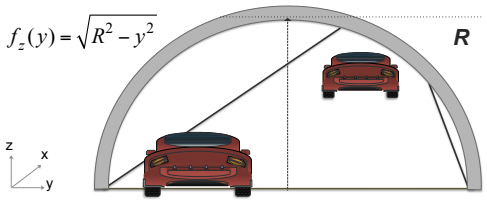

Fig. 2: Tunnel model for a semicircular boundary function.

to the projections of the vectors on the $y-z$ plane: $\tilde{\mathbf{r}}_{j,zy}^{tx} \cdot \hat{\mathbf{n}} = \tilde{\mathbf{r}}_{k,zy}^{rx} \cdot \hat{\mathbf{n}}$. When the projection of both Tx and Rx coincide, the additional condition is given by $\tilde{\mathbf{r}}_{k,zy}^{rx} \cdot \hat{\mathbf{n}} = |\tilde{\mathbf{r}}_{k,zy}^{rx}|$. For the particular case of the semicircular tunnel $f_z(y) = \sqrt{R^2 - y^2}$, the above equations lead to the following coordinates for the reflection point location:

$$y_{cr}(j,k) = \frac{R(y_j^{tx} + y_k^{rx})}{\sqrt{(y_j^{tx} + y_k^{rx})^2 + (z_j^{tx} + z_k^{rx})^2}},$$

and $z_{cr}(j,k) = \sqrt{R^2 - y_{cr}(j,k)^2}$. It can be proved that for any pair of antennas, there is only one reflection point ($q = 0$ for ground reflection and $q = 1$ for tunnel reflection). The distances from each antenna to the plane of reflection are thus given by: $\bar{d}_{j,k} = \sqrt{(y_j^{tx} - y_{cr}(j,k))^2 + (z_j^{tx} - z_{cr}(j,k))^2}$, and $\bar{d}_{k,j} = \sqrt{(y_k^{tx} - y_{cr}(j,k))^2 + (z_k^{tx} - z_{cr}(j,k))^2}$. Therefore the total distance travelled by the tunnel reflection is given by $d_{j,k}^{(1)} = \sqrt{(x_j^{tx} - x_k^{rx})^2 + (\bar{d}_{k,j} + \bar{d}_{j,k})^2}$. From these expressions, the parameters $\cos\beta_1 = d_{j,k}/d_{j,k}^{(1)}$ and $\sin\beta_1 = (\bar{d}_{j,k} + \bar{d}_{k,j})/d_{j,k}^{(1)}$ are drawn out.

IV. MIMO Model

The general MIMO model considering the set of transmit antennas $\mathcal{T}_x$ and the set of receiving antennas $\mathcal{R}_x$, as well as their respective transmit and receive beam-forming arrays $\mathbf{G}_{tx}$ and $\mathbf{G}_{rx}$, can be written as follows:

$$\mathbf{w} = \mathbf{G}_{rx}\mathbf{H}\mathbf{G}_{tx}\mathbf{s} + \mathbf{v}, \quad (6)$$

where $\mathbf{s} = [s(0), s(1), \ldots, s(|\mathcal{T}_x| - 1)]^T$ is the vector of transmitted symbols across the different antennas, $(\cdot)^T$ denotes the transpose operator, and $|\cdot|$ denotes the set cardinality operator. The vector $\mathbf{v}$ represents a zero-mean additive circular complex Gaussian noise $\mathbf{v} \sim \mathcal{CN}(\mathbf{0}_{|\mathcal{R}_x|}, \sigma_v^2 \mathbf{I}_{|\mathcal{R}_x|})$, where $\mathcal{CN}(\mathbf{m}, \mathbf{\Delta})$ denotes a complex circular Gaussian distribution with mean $\mathbf{m}$ and covariance matrix $\mathbf{\Delta}$, $\mathbf{I}_n$ denotes the identity matrix of order n, and $\mathbf{0}_n$ and $\mathbf{1}_n$, the respective column vectors of zeroes and ones of length n. $\mathbf{H}$ is the MIMO channel matrix of size $|\mathcal{R}_x| \times |\mathcal{T}_x|$ which corresponds to the transpose of the matrix formed by the elements $h_{j,k}$, and $\mathbf{x}$ is the vector of received symbols.

A. Capacity and SVD analysis

The capacity of MIMO systems is defined as [10]

$$C = \log_2 \det\left|\mathbf{I} + \mathbf{H}\mathbf{H}^H/|\mathcal{T}_x|\right|, \quad (7)$$

where $\det|\cdot|$ is the determinant operator and $(\cdot)^H$ the Hermitian transpose operator. The singular value decomposition (SVD) of the channel matrix can be expressed as:

$$\mathbf{H} = \mathbf{U}\mathbf{\Sigma}\mathbf{V}, \tag{8}$$

where $\mathbf{U}$ and $\mathbf{V}$ are the unitary matrices containing the receive and transmit optimum beamforming vectors. The diagonal matrix $\mathbf{\Sigma}$ contains the singular values of the channel.

V. Performance model

A. MRC receive diversity

Maximum-ratio combining (MRC) at the receiver side is implemented by using . This leads to the formula of signal to noise ratio (SNR):

$$\eta = \alpha \sum_{j\in\mathcal{R}_x} \left| \sum_{k\in\mathcal{T}_x} \left(\frac{e^{2\pi i \tilde{d}_{j,k}}}{\tilde{d}_{j,k}} + \sum_q \Gamma_q \frac{e^{2\pi i \tilde{d}^{(q)}_{j,k}}}{\tilde{d}^{(q)}_{j,k}} \right) \right|^2, \tag{9}$$

where $\alpha = \frac{P_T G_T G_R}{|\mathcal{T}_x|(4\pi)^2\sigma_v^2}$.

B. ECG receive diversity

Equal-gain combining refers to the scheme where all the received signals are simply averaged instead of being weighted by each measured channel component. The SNR expression for the ECG technique results to be:

$$\eta = \alpha \left| \sum_{k\in\mathcal{R}_x} \sum_{j\in\mathcal{T}_x} \left(\frac{e^{2\pi i \tilde{d}_{j,k}}}{\tilde{d}_{j,k}} + \sum_q \Gamma_q \frac{e^{2\pi i \tilde{d}^{(q)}_{j,k}}}{\tilde{d}^{(q)}_{j,k}} \right) \right|^2. \tag{10}$$

C. Full diversity

As benchmark of the proposed schemes, we detail here a solution where all channel components are used ideally for diversity combining. This scheme is called here "full diversity" (FD). This leads to the following formula for the SNR:

$$\eta = \alpha \sum_{k\in\mathcal{R}_x} \sum_{j\in\mathcal{T}_x} \left| \frac{e^{2\pi i \tilde{d}_{j,k}}}{\tilde{d}_{j,k}} + \sum_q \Gamma_q \frac{e^{2\pi i \tilde{d}^{(q)}_{j,k}}}{\tilde{d}^{(q)}_{j,k}} \right|^2. \tag{11}$$

D. Antenna selection

In our previous paper we proposed a modified scheme based on antenna selection. The idea behind this proposal is that not always having all the available Tx and Rx antennas is beneficial for improved LOS performance. There could be configurations of multiple antennas that can experience deeper fades than other configurations. Therefore, in the proposed scheme, both the optimum transmit and receive antenna sets can be calculated to maximize performance as follows:

$$\eta_{max} = \max_{\mathcal{T}_x,\mathcal{R}_x} \eta, \tag{12}$$

where

$$\eta = \tilde{\alpha} \sum_{k\in\mathcal{R}_x} \delta_k \sum_{j\in\mathcal{T}_x} \xi_{j,k} h_{j,k}.$$

The values $\tilde{\alpha} = \alpha$, $\delta_k = 1$ and $\xi_{j,k} = h^*_{j,k}$ refer to full diversity. The values $\tilde{\alpha} = \alpha$, $\delta_k = \sum_{j\in\mathcal{T}_k} h^*_{j,k}$ and $\xi_{j,k} = 1$ correspond to MRC. Finally, the values $\tilde{\alpha} = \alpha \sum_{k\in\mathcal{R}_x} \sum_{j\in\mathcal{T}_x} h^*_{j,k}$, $\delta_k = 1$ and $\xi_{j,k} = 1$ correspond to EGC. The optimization in (12) is conducted using an exhaustive search algorithm.

VI. Evaluation

Setup: Consider an in-tunnel 2-vehicle configuration with $N_{Tx} = N_{Rx} = 4$ antennas and variable distance between cars. The antennas on each car are distributed in two arrays placed at two different heights, namely $z_1 = 2$m and $z_2 = 0.7$m. Both arrays are parallel on the y-axis, and separated by a shift of 0.2m towards the front/back of the following/lead car. The width of the cars is 1.5m, over which the antennas of the arrays are regularly spaced. Both vehicles are assumed to be aligned to the center of a semicircular tunnel with radius $R = 5$m. The rest of simulation parameters is given in Table I.

Results: Fig. 3 to Fig. 5 present the results of the combination of different transmit and receive antennas using various processing algorithms, namely, MRC, EGC, FD and antenna selection. Some of the figures include the performance without the influence of tunnel or ground reflections. The idea is to evaluate how/when the fades or peaks appears in the received signal as a consequence of the destructive/constructive interference of the multiple reflection components. The "2-ray" curves denotes the case with only ground reflection components (or no tunnel reflections), while the "FSL" curves denotes the baseline case of free space loss (or no reflections at all).

Fig. 3 shows both the maximum and minimum eigenvalues, as described in Eq. (8), for the channel matrix versus distance between vehicles using a 6GHz center frequency. These results suggest the ability of the MIMO systems to achieve parallel information transmission (diversity) is relatively good. Yet, because of the very low minimum eigenvalues observed, a full rank performance might not be achieved. Note that these MIMO tools analysis are more intended for fading channels, instead of the analysis here presented for deterministic (multiple) rays. As for the tunnel influence, the results shows a high frequency envelope-like influence which is due to the tunnel reflection component. Since we selected $R = 5$ meters as radius, the variation on the composite of direct and ground reflected components is much higher. The results for an equivalent V2V configuration without tunnel reflection can be found in our previous publication in [9].

Fig. 4 presents the received signal strength (in dB) versus inter-vehicle distance for various MIMO transmission options under different receiver combining schemes. It reveals antenna selection as better configuration in terms signal quality on the receiver side. It also assess the performance when considering different antenna polarization settings, namely, vertical, horizontal and cross-polarization; denoted by "h","v" and "x", respectively, within the legend of the curves. The results inform not much difference between the horizontal and vertical polarization options. But, promising results for the cross-polarization setting, particularly, in terms of the reduction (smoothing) of fades for the 4x4 configuration. In addition, the effect of dielectric losses of asphalt on the 4x4 EGC horizontal solution (denoted by "4x4EGCh*") seem to be more visible than in the results of our previous work in [9].

Fig. 5 show the capacity results of the channel (according to Eq.(7)) versus inter-vehicle distance for several antenna

TABLE I: Notation and simulation parameters

Variable	Meaning	value
d_{veh}	Intra-vehicular distance	1-20
h_1	height of top antennas	2
h_2	height of bottom antennas	0.7
v_w	vehicle width	1.5
$\epsilon_{r,0}$	rel. permittivity of floor (asphalt) [17]	4
$\epsilon_{r,1}$	rel. permittivity of tunnel walls (concrete) [12]	8.92
λ	wavelength	0.05m (6GHz)
σ_0	conductivity of floor (asphalt) [17]	0.02
σ_1	conductivity of tunnel walls (concrete) [12]	0.046
$h_{j,k}$	channel between antenna j and antenna k	(3)
N_{Tx}	Number of Tx antennas	$1,..,4$
N_{Rx}	Number of Rx antennas	$1,..,4$
P_T	Tx Power	1
Γ_q	Reflection coefficient	(5)
$\mathbf{s}$	Transmitted signal across antennas	QAM
G_T, G_R	Tx and Rx Antenna gains	1
$\mathcal{R}_x$	Set of antennas used at the Rx side	$\{1,..,4\}$
$\mathcal{T}_x$	Set of antennas used at the Tx side	$\{1,..,4\}$

configurations at both sides. The results show that in our particular setting, the conventional diversity combining techniques (successful against fading) sometimes reduce their performance. The figure also shows the effect of scattering using the V2V stochastic model in [18] with a Rice factor of 3dB. The results suggest that our LOS model provides good approximation when Rice factors are relatively low. As for Fig. 6, it shows the results for the signal strength versus inter-vehicle distance in the range of 10 to 1000m in log-scale.

In line with our prior work in [9], these results show that, in general, EGC provides the higher signal values. However, MRC and FD based solutions perform better against fades, thus providing a smoothing effect. Finally, the antenna selection scheme provides the best option in terms of signal strength at every single point of the inter-vehicular distance range.

VII. Conclusions

This paper has presented the evaluation of the effects of reflections both on ground and on the inner walls of a tunnel on the V2V LOS MIMO systems. The multi-ray reflection model here presented is an extension of our prior work on LOS MIMO performance under the (self-)interference effects of ground reflections. It is observed that the reflection component from the inner wall of the tunnel generates a higher frequency oscillation interference pattern that is superimposed on the lower frequency interference pattern of the conventional ground reflection results. The multiple antenna processing algorithms evaluated have shown fade mitigation features that allow the system to control the destructive interference from the multiple reflections. EGC has shown the maximum signal gains at different values of inter-vehicular distances, but it is still subject to some large signal dropouts. The MRC solutions seem to be more resistant to the fades as compared to the EGC solution, but on the opposite side, they do not achieve the same largest gain. The solution for full diversity builds upon the MRC solutions to provide further resistance to fades, but also less reduced gain in signal strength. Moreover, the full diversity solutions really seems to smooth out any extreme signal excursion, including the effects of tunnel reflections, whose undulations at higher frequency also seem to be reduced.

Acknowledgments

This work was partially supported by National Funds through FCT/MCTES (Portuguese Foundation for Science and Technology), within the CISTER Research Unit (UIDB/04234/2020); by the Operational Competitiveness Programme and Internationalization (COMPETE 2020) under the PT2020 Agreement, through the European Regional Development Fund (ERDF), and by national funds through the FCT, within project POCI-01-0145-FEDER032218 (5GSDN); by the FCT and the EU ECSEL JU under the H2020 Framework Programme, within project ECSEL/0002/2019, JU grant nr. 876038 (InSecTT). Disclaimer: The document reflects only the author's view and the Commission is not responsible for any use that may be made of the information it contains; by FCT and the ESF (European Social Fund) through the Regional Operational Programme (ROP) Norte 2020, under PhD grant 2020.06685.BD.; also by the Portuguese National Innovation Agency (ANI) and FCT, under the CMU Portugal partnership, through the Operational Competitiveness Programme and Internationalization (COMPETE 2020) under the PT2020 Partnership Agreement, through the European Regional Development Fund (ERDF), within project grant nr. 45912 (FLOYD).

References

[1] D. Matolak "Modeling the vehicle-to-vehicle propagation channel: A review" *Radio Science,* vol. 49, no. 9, pp. 721-736, Sept. 2014.

[2] P. Liu, B. Ai, D. Matolak, R. Sun, and Y. Li. 5-GHz vehicle-to-vehicle channel characterization for example overpass channels. *IEEE Trans. on Vehicular Technology*, 65(8):5862–5873, 2015.

[3] R. Sun, D. Matolak, and P. Liu. Parking garage channel characteristics at 5 GHz for V2V applications. In *2013 IEEE 78th Vehicular Technology Conference (VTC Fall)*, pages 1–5. IEEE, 2013.

[4] L. Bernadó, A. Roma, A. Paier, T. Zemen, N. Czink, J. Karedal, A. Thiel, F. Tufvesson, A. F. Molisch, and C. F. Mecklenbrauker. In-tunnel vehicular radio channel characterization. In *2011 IEEE 73rd Vehicular Technology Conference (VTC Spring)*, pages 1–5. IEEE, 2011.

[5] A. Chehri and P. Fortier. Autonomous vehicles in underground mines, where we are, where we are going? In *2020 IEEE 91st Vehicular Technology Conference (VTC2020-Spring)*, pages 1–5. IEEE, 2020.

[6] E. Adegoke, J. Zidane, E. Kampert, C. R. Ford, S. A. Birrell, and M. D Higgins. Infrastructure wi-fi for connected autonomous vehicle positioning: A review of the state-of-the-art. *Vehicular Communications*, 20:100185, 2019.

[7] C. Rizzo, F. Lera, and J. L. Villarroel. Transversal fading analysis in straight tunnels at 2.4 GHz. In *2013 13th International Conference on ITS Telecommunications (ITST)*, pages 313–318. IEEE, 2013.

[8] N. Avazov, S. R. Islam, D. Park, and K. S. Kwak. Statistical characterization of a 3-d propagation model for v2v channels in rectangular tunnels. *IEEE Antennas and Wireless Propagation Letters*, 16:2392–2395, 2017.

[9] A. H. Farzamiyan, M. G. Gaitán, and R. Sámano-Robles. "A multi-ray analysis of LOS V2V links for multiple antennas with ground reflection," *2020 AEIT International Annual Conference (AEIT)*, pp. 1–6. IEEE.

[10] A. Goldsmith *Wireless Communications*. Cambridge University Press, New York, NY, 2005.

[11] W. Viriyasitavat, M. Boban, H. Tsai, and A. Vasilakos "Vehicular Communications: Survey and Challenges of Channel and Propagation Models" *IEEE Veh. Tech. Mag.,* vol. 10, no. 2, pp. 55-66, June 2015.

[12] M. Gan, Z. Xu, V. Shivaldova, A. Paier, F. Tufvesson, and T. Zemen. A ray tracing algorithm for intelligent transport systems in tunnels. In *2014 IEEE 6th International Symposium on Wireless Vehicular Communications (WiVeC 2014)*, pages 1–5. IEEE, 2014.

[13] M. Yusuf, E. Tanghe, L. Martens, P. Laly, D. P. Gaillot, M. Liénard, P. Degauque, and W. Joseph. Experimental investigation of V2I radio channel in an arched tunnel. In *2019 13th European Conference on Antennas and Propagation (EuCAP)*, pages 1–5. IEEE, 2019.

[14] N. Avazov and M. Pätzold. A novel wideband MIMO car-to-car channel model based on a geometrical semi-circular tunnel scattering model. *IEEE Transactions on Vehicular Technology*, 65(3):1070–1082, 2015.

[15] W.C. Jakes (1974). Microwave Mobile Communications. New York: IEEE Press.

[16] I. M. Besieris "Comments on the Corrected Fresnel Coefficients for Lossy Materials"," *IEEE Ant. and Prop. Mag.*, vol. 53, no. 4, pp. 161-4, 2011.

[17] E.J. Jaselkis, et al. Dielectric properties of Asphalt pavement, Journal of materials in Civil Engineering, No. 15, Vol. 15, 2003, pp. 427-433.

[18] J. T. Gutiérrez-Mena, C. A. Gutiérrez and J. V. Castillo "Geometrical modeling of non-stationary double-Rayleigh fading channels for MIMO vehicle-to-vehicle communications," *2017 IEEE LATINCOM*, Guatemala, 2017, pp. 1-6.

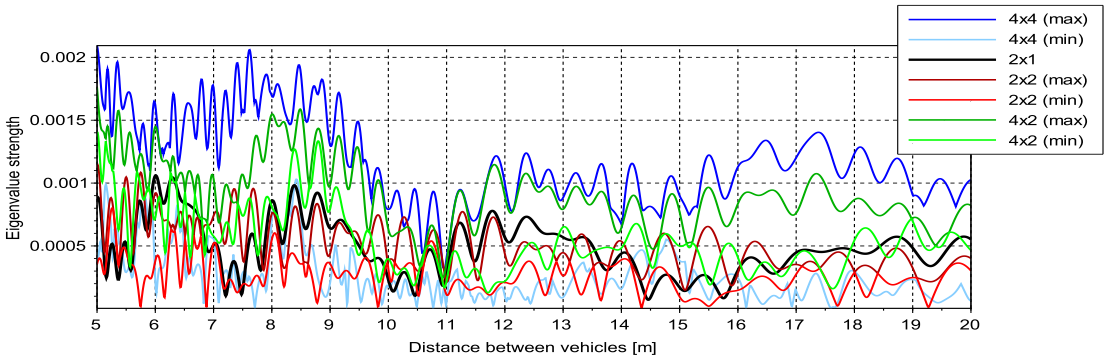

Fig. 3: Maximum and minimum singular values for the channel matrix versus distance between vehicles.

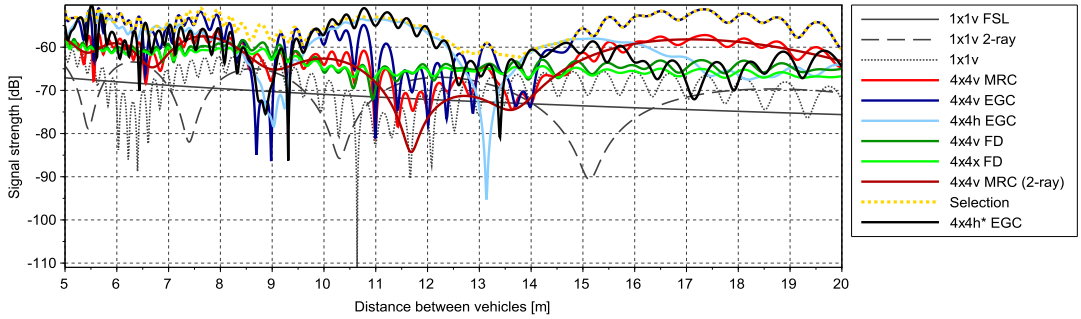

Fig. 4: Received signal strength (dB) vs distance between vehicles for several configurations of multiple antennas at the transmitter and receiver side, considering ground reflected wave propagation, EGC and full diversity.

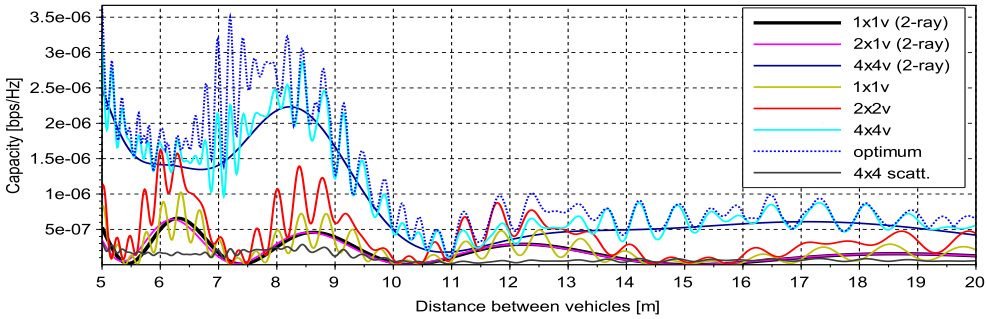

Fig. 5: Capacity (bps/Hz) vs distance between vehicles for several configurations of multiple antennas at the transmitter and receiver side, considering ground reflected wave propagation, EGC and full diversity.

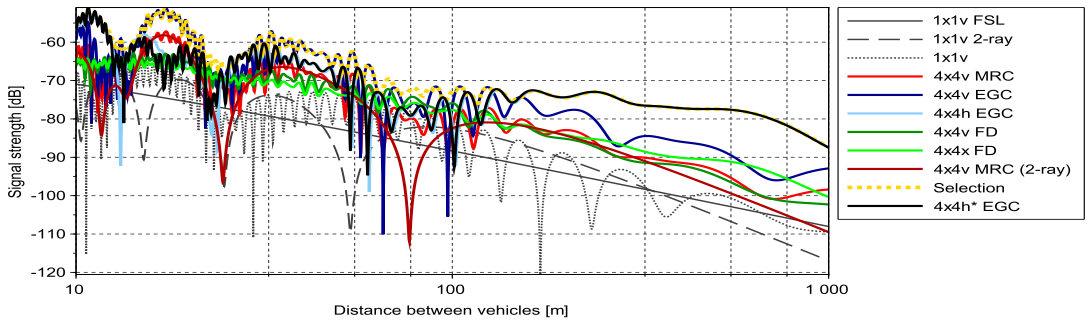

Fig. 6: Received signal strength (dB) vs distance between vehicles for several configurations of multiple antennas at the transmitter and receiver side, considering ground reflected wave propagation, EGC and full diversity.